Erratum: Vector Cross-Product Direction-Finding' with an Electromagnetic Vector-Sensor of Six Orthogonally Oriented...

Article *in* IEEE Transactions on Signal Processing · February 2011

DOI: 10.1109/TSP.2010.2084085 · Source: IEEE Xplore

CITATIONS
56

READS
324

2 authors:

Kainam Thomas Wong
The Hong Kong Polytechnic University
163 PUBLICATIONS **2,804** CITATIONS
SEE PROFILE

Xin Yuan
Nokia Bell Labs
85 PUBLICATIONS **765** CITATIONS
SEE PROFILE

"Vector Cross-Product Direction-Finding" With an Electromagnetic Vector-Sensor of Six Orthogonally Oriented But Spatially Noncollocating Dipoles/Loops

Kainam Thomas Wong, *Senior Member, IEEE*, and Xin Yuan, *Student Member, IEEE*

***Abstract*—Direction-finding capability has recently been advanced by synergies between the customary approach of interferometry and the new approach of "vector cross product" based Poynting-vector estimator. The latter approach measures the incident electromagnetic wavefield for each of its six electromagnetic components, all at one point in space, to allow a vector cross-product between the measured electric-field vector and the measured magnetic-field vector. This would lead to the estimation of each incident source's Poynting-vector, which (after proper norm-normalization) would then reveal the corresponding Cartesian direction-cosines, and thus the azimuth-elevation arrival angles. Such a "vector cross product" algorithm has been predicated on the measurement of all six electromagnetic components at one same spatial location. This physically requires an electromagnetic vector-sensor, i.e., three identical but orthogonally oriented electrically short dipoles, plus three identical but orthogonally oriented magnetically small loops—all spatially *collocated* in a point-like geometry. Such a complicated "vector-antenna" would require exceptionally effective electromagnetic isolation among its six component-antennas. To minimize mutual coupling across these collocated antennas, considerable antennas-complexity and hardware cost could be required. Instead, this paper shows how to apply the "vector cross-product" direction-of-arrival estimator, even if the three dipoles and the three loops are located *separately* (instead of collocating in a point-like geometry). This new scheme has great practical value, in reducing mutual coupling, in simplifying the antennas hardware, and in sparsely extending the spatial aperture to refine the direction-finding accuracy by orders of magnitude.**

***Index Terms*—Antenna array mutual coupling, antenna arrays, aperture antennas, array signal processing, direction of arrival estimation, diversity methods, nonuniformly spaced arrays, polarization.**

I. Introduction

A. The Six-Component Electromagnetic Vector Sensor (EMVS) for Direction Finding

A SIX-COMPONENT electromagnetic vector-sensor consists of three identical, but orthogonally oriented, electrically short *dipoles*, plus three identical but orthogonally oriented magnetically small *loops*—all **spatially collocated** in a point-like geometry. This electromagnetic vector-sensor aims to distinctly measure all three Cartesian components of the incident electric field and all three Cartesian components of the incident magnetic field, as a 6×1 vector, **at one spatial location** and at one time-instant.

Such an electromagnetic vector-sensor's array manifold may be idealized, by overlooking all mutual coupling among its six **collocated** constituent antennas. This idealized array manifold would be a concatenation of the 3×1 electric-field vector $\mathbf{e}$ with the 3×1 magnetic-field vector $\mathbf{h}$, to be [4]

$$\mathbf{a} \stackrel{\text{def}}{=} \begin{bmatrix} \mathbf{e} \\ \mathbf{h} \end{bmatrix} \stackrel{\text{def}}{=} \begin{bmatrix} e_x \\ e_y \\ e_z \\ h_x \\ h_y \\ h_z \end{bmatrix} \stackrel{\text{def}}{=} \underbrace{\begin{bmatrix} \cos\phi\cos\theta & -\sin\phi \\ \sin\phi\cos\theta & \cos\phi \\ -\sin\theta & 0 \\ -\sin\phi & -\cos\phi\cos\theta \\ \cos\phi & -\sin\phi\cos\theta \\ 0 & \sin\theta \end{bmatrix}}_{\stackrel{\text{def}}{=}\boldsymbol{\Theta}(\boldsymbol{\theta},\boldsymbol{\phi})} \underbrace{\begin{bmatrix} \sin\gamma e^{j\eta} \\ \cos\gamma \end{bmatrix}}_{\stackrel{\text{def}}{=}\mathbf{g}} \tag{1}$$

where $\theta \in [0, \pi]$ denotes the incident source's elevation-angle measured from the positive z axis, $\phi \in [0, 2\pi)$ symbolizes the azimuth-angle measured from the positive x axis, $\gamma \in [0, \pi/2]$ refers to the auxiliary polarization angle, and $\eta \in [-\pi, \pi)$ represents the polarization phase difference. Note that $\boldsymbol{\Theta}(\theta, \phi)$ depends only on the arrival-angles, whereas $\mathbf{g}$ depends only on the polarization-parameters. Also, $||\mathbf{e}|| = ||\mathbf{h}|| = 1, \forall(\theta, \phi, \gamma, \eta)$.

By measuring the incident electromagnetic wavefield explicitly in terms of its six individual electromagnetic components, the electromagnetic vector-sensor physically gathers the full data necessary to estimate the Poynting-vector $\mathbf{p}$, via a simple vector-cross-product between the measured electric-field vector and the measured magnetic-field vector. This estimated Poynting-vector, when normalized with respect to its Frobenius norm $||\cdot||$, gives the incident source's Cartesian direction-cosines (and hence the incident source's elevation-angle and azimuth-angle). Mathematically

$$\mathbf{p} \stackrel{\text{def}}{=} \begin{bmatrix} p_x \\ p_y \\ p_z \end{bmatrix} = \frac{\mathbf{e} \times \mathbf{h}^*}{||\mathbf{e}|| \cdot ||\mathbf{h}^*||} = \begin{bmatrix} u \\ v \\ w \end{bmatrix} \stackrel{\text{def}}{=} \begin{bmatrix} \sin\theta & \cos\phi \\ \sin\theta & \sin\phi \\ \cos\theta & \end{bmatrix} \tag{2}$$

Manuscript received March 15, 2010; accepted September 17, 2010. Date of publication October 07, 2010; date of current version December 17, 2010. The associate editor coordinating the review of this manuscript and approving it for publication was Dr. Philipe Ciblat. This work was supported by the Hong Kong Polytechnic University's Internal Competitive Research Grant #G-YG38.

The authors are with the Department of Electronic and Information Engineering, Hong Kong Polytechnic University, Hung Hom, Kowloon, Hong Kong (e-mail: ktwong@ieee.org).

Color versions of one or more figures in this paper are available online at http://ieeexplore.ieee.org.

Digital Object Identifier 10.1109/TSP.2010.2084085

where the superscript * denotes complex conjugation, $\times$ symbolizes the vector cross-product operator, with u, v, and w representing the impinging source's direction-cosines respectively along the x axis, the y axis, and the z axis.

The unique array-manifold in (1) has been much exploited by various eigenstructure-based direction-finding schemes [3], [5]–[16], [19], [21]–[37], [40]–[45], [47].

Many are the advantages offered by this six-component electromagnetic vector-sensor to arrival-angle estimation:

1) In a multisource scenario, each source's three Cartesian direction-cosine estimates (and thus each source's azimuth-angle estimate and elevation-angle estimate) can be automatically paired without further postprocessing.
2) Like other diversely polarized antenna-arrays, the electromagnetic vector-sensor can resolve incident sources on account of the sources' polarization-difference, in addition to their azimuth/elevation angular differences.
3) The "vector-cross-product" approach of direction-finding in (2) can complement the customary interferometry approach of DOA-estimation, which is based on the spatial phase-delay across displaced antennas. Creative synergy between these two approaches has produced several novel capabilities:
   a) The direction-of-arrival estimation accuracy can be improved by orders of magnitude, by extending the spatial aperture, with*out* incurring ambiguity in the direction-of-arrival estimates and with*out* requiring additional antennas [13], [14].
   b) The directions-of-arrival may be estimated with*out* prior knowledge/estimation of the nominal/actual geometric array-grid and with*out* any calibration-source, thereby easing "real-world" deployment [12].
   c) No prior coarse estimate is needed to initiate the MUltiple SIgnal Classification (MUSIC) iterative parameter-estimation routine. Instead, MUSIC can now "self-initiates" its iteration [15].
   d) Blind geolocation, beamforming, and interference-rejection are possible for frequency-hopping sources of unknown and arbitrary hop-sequences and directions-of-arrival [16].

B. An Electromagnetic Vector-Sensor of Spatially Noncollocating Component-Antennas

Unrealistically presumed by the algorithms cited in Section I-A, however, is *negligible* mutual coupling across the six **collocated** antennas that constitute the electromagnetic vector-sensor. Mutual coupling could be reduced but never entirely avoided, and only by intricate electromagnetic isolation, that would categorically complicate the antenna implementation and would thus sky-rocket the hardware cost [46]. Instead, this proposed scheme bypasses this mutual coupling problem, by spatially **displacing** the six component-antennas and showing how to modify the "vector-cross-product" Poynting-vector estimator accordingly. That is, this proposed method will retain all advantages mentioned in Section I-A of *collocated* vector-sensor direction-finding, despite spatially *separating* the six component-antennas here. Furthermore, *additional* advantages become available, as explained here.

4) As the six constituent antennas now span an extended spatial aperture (instead of collocating at one point), the resulting antennas have improved azimuth-elevation spatial resolution. That is, the present scheme spatially extends the geometric aperture, with*out* additional antenna.
5) As aforementioned, spatially separation of the six component-antennas reduces their mutual coupling, thereby saving the cost to implement electromagnetic isolation.

The key question now is: Across the **spatially displaced** component-antennas, spatial phase shifts exist, invalidating the array manifold of (1) and nullifying the vector cross-product Poynting-vector estimation in (2). To these problems, this paper will advance a class of array-configurations to spatially space the six constituent antennas of the now-spread electromagnetic vector-sensor, such that the vector cross-product estimator would still work—and would work better, indeed.[1][2]

II. Array Manifold for the New Electromagnetic Vector-Sensor With Noncollocated Component-Antennas

The following notation will be used: The symbol E_x refers to the dipole oriented along the x axis, similarly for E_y and E_z. The symbol H_x corresponds to the loop oriented along the x axis, analogously for H_y and H_z. The symbols $\tilde{\theta}, \tilde{\phi}, \Delta_{x,y}$ signify, respectively, the elevation-angle, the azimuth-angle, and the distance of E_y relative to E_x. Similarly, $\Delta_{y,z}$ defines the distance of E_z from E_y.

This work will show the following:

The "vector-cross-product" estimator remains applicable for an electromagnetic vector-sensor of spatially noncollocated component-antennas, if[3]

A) The x, y, and z axis oriented **dipoles** are all placed on a straight line, with a spacing $\Delta_{x,y}$ between the first two dipoles, and a spacing $\Delta_{y,z}$ between the last two dipoles.
B) The x-, y, and z axis oriented **loops** are placed in an order opposite to that in $\{\mathrm{A}\}$, on another straight line in parallel to the first straight line,[4] with a spacing $\Delta_{x,y}$ between the first two loops, and a spacing $\Delta_{y,z}$ between the last two loops.

[1][17] has previously shown how the vector-cross-product DOA-estimator remains fully applicable, for a dipole-triad that is displaced from a loop-triad. However, the three dipoles there remain spatially *co*llocated among themselves; and so do the three loops among themselves. Hence, mutual coupling, though reduced in [17], remains very substantial. In contrast, the present scheme allows each of six constituent antennas to occupy its distinct location, away from all other five component-antennas.

[2]Estimation accuracy bounds are derived in [20] for a spatially extended electromagnetic vector-sensor under certain specific array-configurations; however, *no algorithm* is presented therein. [38], [39] advance hardware implementations of a spatially extended electromagnetic vector-sensor, but again no algorithm. Original to the present work is the modification of the vector cross-product estimator to adopt to a spatially extended electromagnetic vector-sensor.

[3]These constitute a sufficient condition, maybe not a necessary condition.

[4]If $\bar{\theta} = \pi/2$, the aforementioned two array-axes will be parallel to the x-y Cartesian plane. If $\bar{\phi} = \pi/2$ additionally, the two lines are parallel to the y axis; if $\bar{\phi} = 0$ instead, the two lines lie in parallel to x axis.

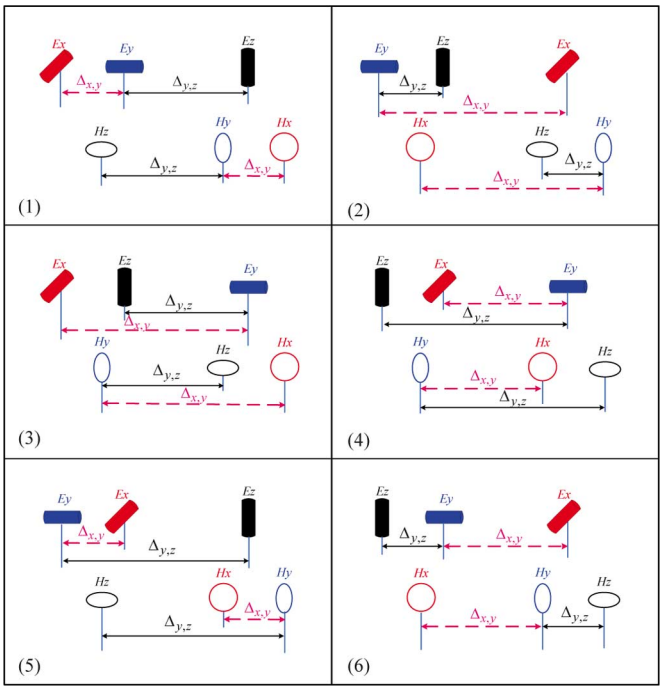

Fig. 1. Six permutations to place the six orthogonally dipoles/triads on two parallel lines, which may lie arbitrarily in three-dimensional space as shown in Fig. 2.

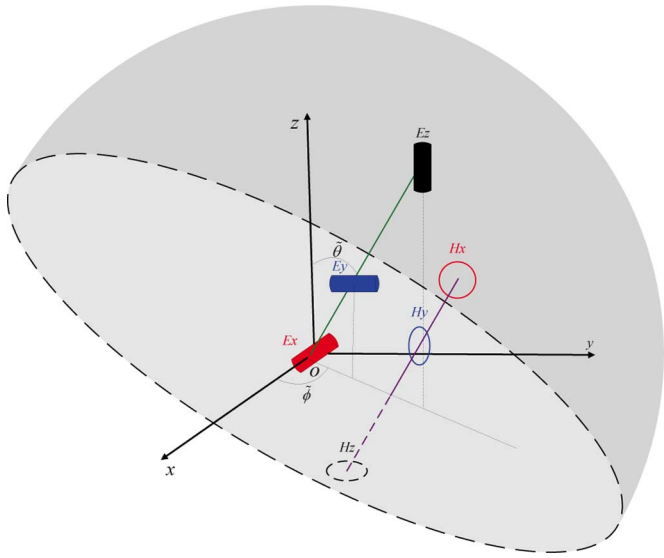

Fig. 2. Spatial geometry, showing for the dipoles/loops permutation case (1) in Fig. 1.

For the spatially *non*-collocating electromagnetic vector-sensor aforementioned, the array manifold is no longer (1), but (3), shown at the bottom of the page. In which, $\tilde{u} = \sin(\tilde{\theta})\cos(\tilde{\phi})$, $\tilde{v} = \sin(\tilde{\theta})\sin(\tilde{\phi})$, $\tilde{w} = \cos(\tilde{\theta})$, and $\odot$ symbolizes the element-wise multiplication between two vectors.

The spatial support-region is hemispherical, with the hemispherical base perpendicular to the two array-axes, as in Fig. 2.[5] In (3), the ℓth element of $\mathbf{d}(\theta,\phi)$ represents the ℓth component-antenna's spatial phase-factor, whereas the ℓth element of $\mathbf{a}$ gives the ℓth component-antenna's gain/phase/polarization response. Note the antisymmetry in the exponents of E_y and E_z, versus the exponents of H_y and H_z. This will be critical to the success of the proposed scheme.

[5]In the special case of the two parallel lines parallel to the x axis, the spatial support-region for the estimates would be either the right or the left hemisphere. If the two parallel lines are parallel to the y axis, the spatial support-region would be either the front or the back hemisphere. If parallel to the z axis, the spatial support-region for the estimates would be either the upper or the lower hemisphere.

III. A New "Vector-Cross-Product" Direction-Finding Algorithm

In all eigen-based "vector-cross-product" direction-finding schemes cited in Section II, an intermediate algorithmic step would estimate each incident source's steering vector, but correct to only within an *un*known complex-value scalar c.[6] That is, available (in each algorithm for each incident emitter)[7] is the estimate $\hat{\mathbf{a}} \approx c\mathbf{a}$, from which θ and ϕ are to be estimated. (This approximation becomes a equality in noiseless or asymptotic cases.) The question now is whether $\hat{\tilde{\mathbf{a}}} \approx c\tilde{\mathbf{a}}$ suffices to estimate θ and ϕ unambiguously, where $\tilde{\mathbf{a}}$ denotes the spatially extended (3), instead of the collocated (1).

The answer is "yes"; and the following shows why and how. Cross-multiply $c\tilde{\mathbf{e}}$ and $c\tilde{\mathbf{h}}$ to give

$$c\tilde{\mathbf{e}} \times (c\tilde{\mathbf{h}})^* = |c|^2 e^{j\frac{2\pi}{\lambda}(x_h u + y_h v + z_h w)} \begin{bmatrix} u & e^{-j\frac{2\pi}{\lambda}[(2\Delta_{x,y}+\Delta_{y,z})(\tilde{u}u+\tilde{v}v+\tilde{w}w)]} \\ v & e^{-j\frac{2\pi}{\lambda}[(\Delta_{x,y}+\Delta_{y,z})(\tilde{u}u+\tilde{v}v+\tilde{w}w)]} \\ w & e^{-j\frac{2\pi}{\lambda}\Delta_{x,y}(\tilde{u}u+\tilde{v}v+\tilde{w}w)} \end{bmatrix}. \quad (4)$$

[6]For example, see step {2c.} in Section IV-A, which reviews the key algorithmic steps in the *Uni-Vector-Sensor ESPRIT* method of [6].

[7]This does NOT presume only a single incident source. Multiple, possibly cross-correlated/broadband/time-varying sources can be handled. For details, please refer to those references directly.

$$\tilde{\mathbf{a}} \overset{\text{def}}{=} \begin{bmatrix} \tilde{\mathbf{e}} \\ \tilde{\mathbf{h}} \end{bmatrix} \overset{\text{def}}{=} \underbrace{\begin{bmatrix} 1 \\ e^{-j\frac{2\pi}{\lambda}\Delta_{x,y}(\tilde{u}u+\tilde{v}v+\tilde{w}w)} \\ e^{-j\frac{2\pi}{\lambda}[\Delta_{x,y}(\tilde{u}u+\tilde{v}v+\tilde{w}w)+\Delta_{y,z}(\tilde{u}u+\tilde{v}v+\tilde{w}w)]} \\ e^{-j\frac{2\pi}{\lambda}(x_h u+y_h v+z_h w)} \\ e^{-j\frac{2\pi}{\lambda}(x_h u+y_h v+z_h w)} e^{j\frac{2\pi}{\lambda}\Delta_{x,y}(\tilde{u}u+\tilde{v}v+\tilde{w}w)} \\ e^{-j\frac{2\pi}{\lambda}(x_h u+y_h v+z_h w)} e^{j\frac{2\pi}{\lambda}[\Delta_{x,y}(\tilde{u}u+\tilde{v}v+\tilde{w}w)+\Delta_{y,z}(\tilde{u}u+\tilde{v}v+\tilde{w}w)]} \end{bmatrix}}_{\overset{\text{def}}{=}\mathbf{d}(\theta,\phi)} \odot \underbrace{\begin{bmatrix} e_x \\ e_y \\ e_z \\ h_x \\ h_y \\ h_z \end{bmatrix}}_{\mathbf{a}}. \quad (3)$$

Next, normalize (4) according to its Frobenius norm

$$\frac{(c\tilde{\mathbf{e}})\times(c\tilde{\mathbf{h}})^*}{\|(c\tilde{\mathbf{e}})\times(c\tilde{\mathbf{h}})^*\|} = e^{j\frac{2\pi}{\lambda}(x_h u+y_h v+z_h w)} \begin{bmatrix} u & e^{-j\frac{2\pi}{\lambda}[(2\Delta_{x,y}+\Delta_{y,z})(\tilde{u}u+\tilde{v}v+\tilde{w}w)]} \\ v & e^{-j\frac{2\pi}{\lambda}[(\Delta_{x,y}+\Delta_{y,z})(\tilde{u}u+\tilde{v}v+\tilde{w}w)]} \\ w & e^{-j\frac{2\pi}{\lambda}\Delta_{x,y}(\tilde{u}u+\tilde{v}v+\tilde{w}w)} \end{bmatrix} \stackrel{\text{def}}{=} \mathbf{q}.$$

To ease subsequent exposition, assume *momentarily* that the two array-axes are parallel to one of the Cartesian axis.

A. If the Two Array-Axes are Parallel to the x Axis

This special case has $\tilde{\theta}=\pi/2$ and $\tilde{\phi}=0$; hence, $\mathbf{q}$ degrades to

$$\mathbf{q}_x \stackrel{\text{def}}{=} e^{j\frac{2\pi}{\lambda}x_h u}\begin{bmatrix} u & e^{-j\frac{2\pi}{\lambda}(2\Delta_{x,y}+\Delta_{y,z})u} \\ v & e^{-j\frac{2\pi}{\lambda}(\Delta_{x,y}+\Delta_{y,z})u} \\ w & e^{-j\frac{2\pi}{\lambda}\Delta_{x,y}u} \end{bmatrix}.$$

Consider the following two disjoint cases, separately.

1) Suppose $\phi\in[-\pi/2,\pi/2]$: Consequentially, the x axis direction-cosine $u\geq 0, \forall\theta\in[0,\pi]$. Hence

$$\mathbf{q}_x e^{-j\angle[\mathbf{q}_x]_1} = \begin{bmatrix} u & \\ v & e^{j\frac{2\pi}{\lambda}\Delta_{x,y}u} \\ w & e^{j\frac{2\pi}{\lambda}(\Delta_{x,y}+\Delta_{y,z})u} \end{bmatrix} \stackrel{\text{def}}{=} \acute{\mathbf{q}}_x. \quad (5)$$

where $\angle$ denotes the angle of the ensuing entity, and $[\cdot]_i$ symbolizes the ith element of the square-bracketed vector.

The above equation leads to these estimates of the three Cartesian direction-cosines

$$\begin{aligned} \hat{u}_{\text{coarse}} &= [\acute{\mathbf{q}}_x]_1, \\ \hat{v} &= \text{Re}\left\{[\acute{\mathbf{q}}_x]_2\, e^{-j\frac{2\pi}{\lambda}\Delta_{x,y}\hat{u}_{\text{coarse}}}\right\}, \\ \hat{w} &= \text{Re}\left\{[\acute{\mathbf{q}}_x]_3\, e^{-j\frac{2\pi}{\lambda}(\Delta_{x,y}+\Delta_{y,z})\hat{u}_{\text{coarse}}}\right\} \end{aligned} \quad (6)$$

In the above, $\hat{u}_{\text{coarse}}$ is set to $[\acute{\mathbf{q}}_x]_1$, not to $|[\acute{\mathbf{q}}_x]_1|$, to retain the sign of $[\acute{\mathbf{q}}_x]_1$. Similar considerations apply for $\hat{v}$ and $\hat{w}$. The operand, under noiseless or asymptotic conditions, would necessarily be real-value for each inverse-trigonometric operator above. These operands could become complex-value with noise, hence the real-value operators above.

However, the complex-phases in (5) can afford also *fine* estimates of the x axis direction-cosine:

$$\hat{u}_{\text{fine},1} = \frac{\lambda}{2\pi}\frac{1}{\Delta_{x,y}}\angle\left\{\frac{[\acute{\mathbf{q}}_x]_2}{\hat{v}}\right\} \quad (7)$$

$$\hat{u}_{\text{fine},2} = \frac{\lambda}{2\pi}\frac{1}{(\Delta_{x,y}+\Delta_{y,z})}\angle\left\{\frac{[\acute{\mathbf{q}}_x]_3}{\hat{w}}\right\}. \quad (8)$$

These finer-resolution estimates are obtainable, due to the nonzero interantenna spacings of $\Delta_{x,y}$ and $\Delta_{y,z}$, on account of the sparse array-spacing principle. These more accurate estimates are available here for only the x axis direction-cosine, because both $\Delta_{x,y}$ and $\Delta_{y,z}$ are aligned along the x axis. Therefore, the interantenna spacings are sparse along only the x axis, but not along the y axis nor along the z axis.

As $\Delta_{x,y}$ lengthens beyond $\lambda/2$, more than one value may exist of $\hat{u}_{\text{fine},1}$ that satisfy (7). Hence, this more accurate $\hat{u}_{\text{fine},1}$ could be cyclically ambiguous, in contrast to $\hat{u}_{\text{coarse}}$, which is *un*ambiguous but coarser in estimation accuracy. Similar considerations hold for $\hat{u}_{\text{fine},2}$. These several complementary estimates of u in (6), (7), and (8)), they could be synergized by using $\hat{u}_{\text{coarse}}$ to disambiguate $\hat{u}_{\text{fine},1}$ and $\hat{u}_{\text{fine},2}$, to produce an estimate that is both fine in estimation resolution and unambiguous:

$$\hat{u} = \frac{1}{2}\left\{\hat{u}_{\text{fine},1}+m^{\circ}_{x,y}\frac{\lambda}{\Delta_{x,y}}\right\} + \frac{1}{2}\left\{\hat{u}_{\text{fine},2}+m^{\circ}_{x,z}\frac{\lambda}{\Delta_{x,y}+\Delta_{y,z}}\right\} \quad (9)$$

where

$$\begin{aligned} m^{\circ}_{x,y} &= \stackrel{\arg\min}{m_{x,y}}\left|\hat{u}_{\text{coarse}}-\hat{u}_{\text{fine},1}-m_{x,y}\frac{\lambda}{\Delta_{x,y}}\right| \\ m^{\circ}_{x,z} &= \stackrel{\arg\min}{m_{x,z}}\left|\hat{u}_{\text{coarse}}-\hat{u}_{\text{fine},2}-m_{x,z}\frac{\lambda}{\Delta_{x,y}+\Delta_{y,z}}\right| \end{aligned}$$

for

$$\begin{aligned} m_{x,y} &\in \left\{\left\lceil\frac{\Delta_{x,y}}{\lambda}(-1-\hat{u}_{\text{coarse}})\right\rceil, \left\lfloor\frac{\Delta_{x,y}}{\lambda}(1-\hat{u}_{\text{coarse}})\right\rfloor\right\}, \\ m_{x,z} &\in \left\{\left\lceil\frac{\Delta_{x,y}+\Delta_{y,z}}{\lambda}(-1-\hat{u}_{\text{coarse}})\right\rceil, \left\lfloor\frac{\Delta_{x,y}+\Delta_{y,z}}{\lambda}(1-\hat{u}_{\text{coarse}})\right\rfloor\right\} \end{aligned}$$

where $\lceil\alpha\rceil$ refers to the smallest integer not less than α, and $\lfloor\alpha\rfloor$ refers to the largest integer not exceeding α.

However, for $\Delta_{x,y}\leq\lambda$, the spatial aperture is not much extended; hence, simply set $\hat{u}=\hat{u}_{\text{coarse}}$.

Last

$$\begin{aligned} \hat{\phi} &= \arctan\left\{\frac{\hat{v}}{\hat{u}}\right\} \\ \hat{\theta} &= \arccos\{\hat{w}\}. \end{aligned}$$

2) Suppose $\phi\in[\pi/2,3\pi/2]$: Consequentially, $u\leq 0, \forall\theta\in[0,\pi]$. This gives

$$\mathbf{q}_x e^{-j\angle[\mathbf{q}_x]_1} = \begin{bmatrix} -u & \\ -v & e^{j\frac{2\pi}{\lambda}\Delta_{x,y}u} \\ -w & e^{j\frac{2\pi}{\lambda}(\Delta_{x,y}+\Delta_{y,z})u} \end{bmatrix} \stackrel{\text{def}}{=} \acute{\mathbf{q}}_x,$$

$$\begin{aligned} \hat{u}_{\text{coarse}} &= -[\acute{\mathbf{q}}_x]_1 \\ \hat{v} &= \text{Re}\left\{-[\acute{\mathbf{q}}_x]_2\, e^{-j\frac{2\pi}{\lambda}\Delta_{x,y}\hat{u}_{\text{coarse}}}\right\} \\ \hat{w} &= \text{Re}\left\{-[\acute{\mathbf{q}}_x]_3\, e^{-j\frac{2\pi}{\lambda}(\Delta_{x,y}+\Delta_{y,z})\hat{u}_{\text{coarse}}}\right\} \\ \hat{\phi} &= \arctan\left\{\frac{\hat{v}}{\hat{u}}\right\}+\pi \\ \hat{\theta} &= \arccos\{\hat{w}\} \end{aligned}$$

with $\hat{u}_{\text{fine},1}$ remains as in (7), $\hat{u}_{\text{fine},2}$ as in (8), and $\hat{u}$ as in (9).

B. If the Two Array-Axes Are Parallel to the y Axis

This special case has $\tilde{\theta} = \pi/2$ and $\tilde{\phi} = \pi/2$; therefore, $\mathbf{q}$ degrades to

$$\mathbf{q}_y \stackrel{\text{def}}{=} e^{j\frac{2\pi}{\lambda}y_h v}\begin{bmatrix} u & e^{-j\frac{2\pi}{\lambda}(2\Delta_{x,y}+\Delta_{y,z})v} \\ v & e^{-j\frac{2\pi}{\lambda}(\Delta_{x,y}+\Delta_{y,z})v} \\ w & e^{-j\frac{2\pi}{\lambda}\Delta_{x,y}v} \end{bmatrix}.$$

Separately consider the following two disjoint cases.

1) Suppose $\phi \in [0,\pi]$: Hence the y axis direction-cosine $v \geq 0, \forall\theta \in [0,\pi]$. Hence

$$\mathbf{q}_y e^{-j\angle[\mathbf{q}_y]_2} = \begin{bmatrix} u & e^{-j\frac{2\pi}{\lambda}\Delta_{x,y}v} \\ v & \\ w & e^{j\frac{2\pi}{\lambda}\Delta_{y,z}v} \end{bmatrix} \stackrel{\text{def}}{=} \acute{\mathbf{q}}_y \tag{10}$$

$$\hat{v}_{\text{coarse}} = [\acute{\mathbf{q}}_y]_2$$

$$\hat{v}_{\text{fine},1} = -\frac{\lambda}{2\pi}\frac{1}{\Delta_{x,y}}\angle\left\{\frac{[\acute{\mathbf{q}}_y]_1}{\hat{u}}\right\} \tag{11}$$

$$\hat{v}_{\text{fine},2} = \frac{\lambda}{2\pi}\frac{1}{\Delta_{y,z}}\angle\left\{\frac{[\acute{\mathbf{q}}_y]_3}{\hat{w}}\right\} \tag{12}$$

$$\hat{v} = \frac{1}{2}\left\{\hat{v}_{\text{fine},1} + m^{\circ}_{x,y}\frac{\lambda}{\Delta_{x,y}}\right\} + \frac{1}{2}\left\{\hat{v}_{\text{fine},2} + m^{\circ}_{x,z}\frac{\lambda}{\Delta_{x,y}+\Delta_{y,z}}\right\} \tag{13}$$

if $\Delta_{x,y} \leq \lambda$, where

$$m^{\circ}_{x,y} = \stackrel{\arg\min}{m_{x,y}}\left|\hat{v}_{\text{coarse}} - \hat{v}_{\text{fine},1} - m_{x,y}\frac{\lambda}{\Delta_{x,y}}\right|$$

$$m^{\circ}_{x,z} = \stackrel{\arg\min}{m_{x,z}}\left|\hat{v}_{\text{coarse}} - \hat{v}_{\text{fine},2} - m_{x,z}\frac{\lambda}{\Delta_{x,y}+\Delta_{y,z}}\right|$$

for

$$m_{x,y} \in \left\{\left\lceil\frac{\Delta_{x,y}}{\lambda}(-1-\hat{v}_{\text{coarse}})\right\rceil, \left\lfloor\frac{\Delta_{x,y}}{\lambda}(1-\hat{v}_{\text{coarse}})\right\rfloor\right\},$$

$$m_{x,z} \in \left\{\left\lceil\frac{\Delta_{x,y}+\Delta_{y,z}}{\lambda}(-1-\hat{v}_{\text{coarse}})\right\rceil, \left\lfloor\frac{\Delta_{x,y}+\Delta_{y,z}}{\lambda}(1-\hat{v}_{\text{coarse}})\right\rfloor\right\}.$$

However, for $\Delta_{x,y} \leq \lambda$, simply set $\hat{v} = \hat{v}_{\text{coarse}}$.

Also from (10)

$$\hat{u} = \text{Re}\left\{[\acute{\mathbf{q}}_y]_1 e^{j\frac{2\pi}{\lambda}\Delta_{x,y}\hat{v}_{\text{coarse}}}\right\}$$

$$\hat{w} = \text{Re}\left\{[\acute{\mathbf{q}}_y]_3 e^{-j\frac{2\pi}{\lambda}\Delta_{y,z}\hat{v}_{\text{coarse}}}\right\}$$

$$\hat{\phi} = \begin{cases} \arctan\left\{\frac{\hat{v}}{\hat{u}}\right\}, & \text{if} \quad \hat{u} \geq 0 \\ \arctan\left\{\frac{\hat{v}}{\hat{u}}\right\} + \pi, & \text{if} \quad \hat{u} < 0 \end{cases}$$

$$\hat{\theta} = \arccos\{\hat{w}\}.$$

2) Suppose $\phi \in [\pi, 2\pi]$: This implies that the y axis direction-cosine $v \leq 0, \forall\theta \in [0,\pi]$. Therefore

$$\mathbf{q}_y e^{-j\angle[\mathbf{q}_y]_2} = \begin{bmatrix} -u & e^{-j\frac{2\pi}{\lambda}\Delta_{x,y}v} \\ -v & \\ -w & e^{j\frac{2\pi}{\lambda}\Delta_{y,z}v} \end{bmatrix} \stackrel{\text{def}}{=} \acute{\mathbf{q}}_y.$$

$$\hat{v}_{\text{coarse}} = -[\acute{\mathbf{q}}_y]_2$$

$$\hat{u} = \text{Re}\left\{-[\acute{\mathbf{q}}_y]_1\, e^{j\frac{2\pi}{\lambda}\Delta_{x,y}\hat{v}_{\text{coarse}}}\right\}$$

$$\hat{w} = \text{Re}\left\{-[\acute{\mathbf{q}}_y]_3\, e^{-j\frac{2\pi}{\lambda}\Delta_{y,z}\hat{v}_{\text{coarse}}}\right\}$$

$$\hat{\phi} = \begin{cases} \arctan\left\{\frac{\hat{v}}{\hat{u}}\right\}, & \text{if} \quad \hat{u} \geq 0 \\ \arctan\left\{\frac{\hat{v}}{\hat{u}}\right\} + \pi, & \text{if} \quad \hat{u} < 0 \end{cases}$$

$$\hat{\theta} = \arccos\{\hat{w}\}$$

with $\hat{v}_{\text{fine},1}$ remains as in (11), $\hat{v}_{\text{fine},2}$ as in (12), and $\hat{v}$ as in (13).

C. If the Two Array-Axes Are Parallel to the z Axis

This particular case has $\tilde{\theta} = 0$. $\mathbf{q}$ degrades to

$$\mathbf{q}_z \stackrel{\text{def}}{=} e^{j\frac{2\pi}{\lambda}z_h w}\begin{bmatrix} u & e^{-j\frac{2\pi}{\lambda}(2\Delta_{x,y}+\Delta_{y,z})w} \\ v & e^{-j\frac{2\pi}{\lambda}(\Delta_{x,y}+\Delta_{y,z})w} \\ w & e^{-j\frac{2\pi}{\lambda}\Delta_{x,y}w} \end{bmatrix}. \tag{14}$$

Separately consider the following two disjoint cases.

1) Suppose $\theta \in [0,\pi/2]$: This would imply that the z axis direction-cosine $w \geq 0$. Therefore

$$\mathbf{q}_z e^{-j\angle[\mathbf{q}_z]_3} = \begin{bmatrix} u & e^{-j\frac{2\pi}{\lambda}(\Delta_{y,z}+\Delta_{x,y})w} \\ v & e^{-j\frac{2\pi}{\lambda}\Delta_{y,z}w} \\ w & \end{bmatrix} \stackrel{\text{def}}{=} \acute{\mathbf{q}}_z.$$

From the above equation

$$\hat{w}_{\text{coarse}} = [\acute{\mathbf{q}}_z]_3$$

$$\hat{w}_{\text{fine},1} = -\frac{\lambda}{2\pi}\frac{1}{(\Delta_{x,y}+\Delta_{y,z})}\angle\left\{\frac{[\acute{\mathbf{q}}_z]_1}{\hat{u}}\right\} \tag{15}$$

$$\hat{w}_{\text{fine},2} = -\frac{\lambda}{2\pi}\frac{1}{\Delta_{y,z}}\angle\left\{\frac{[\acute{\mathbf{q}}_z]_2}{\hat{v}}\right\} \tag{16}$$

$$\hat{w} = \frac{1}{2}\left\{\hat{w}_{\text{fine},1} + m^{\circ}_{x,z}\frac{\lambda}{\Delta_{x,y}+\Delta_{y,z}}\right\} + \frac{1}{2}\left\{\hat{w}_{\text{fine},2} + m^{\circ}_{y,z}\frac{\lambda}{\Delta_{y,z}}\right\} \tag{17}$$

for $\Delta_{y,z} > \lambda$, where

$$m^{\circ}_{x,z} = \stackrel{\arg\min}{m_{x,z}}\left|\hat{w}_{\text{coarse}} - \hat{w}_{\text{fine},1} - m_{x,z}\frac{\lambda}{\Delta_{x,y}+\Delta_{y,z}}\right|$$

$$m^{\circ}_{y,z} = \stackrel{\arg\min}{m_{y,z}}\left|\hat{w}_{\text{coarse}} - \hat{w}_{\text{fine},2} - m_{y,z}\frac{\lambda}{\Delta_{y,z}}\right|$$

for

$$m_{x,z} \in \left\{\left\lceil\frac{\Delta_{x,y}+\Delta_{y,z}}{\lambda}(-1-\hat{w}_{\text{coarse}})\right\rceil, \left\lfloor\frac{\Delta_{x,y}+\Delta_{y,z}}{\lambda}(1-\hat{w}_{\text{coarse}})\right\rfloor\right\},$$

$$m_{y,z} \in \left\{ \left\lceil \frac{\Delta_{y,z}}{\lambda}(-1-\hat{w}_{\text{coarse}}) \right\rceil, \left\lfloor \frac{\Delta_{y,z}}{\lambda}(1-\hat{w}_{\text{coarse}}) \right\rfloor \right\}.$$

However, for $\Delta_{y,z} \leq \lambda$, simply set $\hat{w} = \hat{w}_{\text{coarse}}$.

Also from (14),

$$\hat{u} = \text{Re}\left\{ [\acute{\mathbf{q}}_z]_1 e^{j\frac{2\pi}{\lambda}(\Delta_{x,y}+\Delta_{y,z})\hat{w}_{\text{coarse}}} \right\}$$
$$\hat{v} = \text{Re}\left\{ [\acute{\mathbf{q}}_z]_2 e^{j\frac{2\pi}{\lambda}\Delta_{y,z}\hat{w}_{\text{coarse}}} \right\}$$
$$\hat{\phi} = \begin{cases} \arctan\left\{\frac{\hat{v}}{\hat{u}}\right\}, & \text{if} \quad \hat{u} \geq 0 \\ \arctan\left\{\frac{\hat{v}}{\hat{u}}\right\} + \pi, & \text{if} \quad \hat{u} < 0 \end{cases}$$
$$\hat{\theta} = \arccos\{\hat{w}\}.$$

2) Suppose $\theta \in [\pi/2, \pi]$: This implies that $w \leq 0$. Therefore

$$\mathbf{q}_z e^{-j\angle[\mathbf{q}_z]_3} = \begin{bmatrix} -ue^{-j\frac{2\pi}{\lambda}(\Delta_{y,z}+\Delta_{x,y})w} \\ -ve^{-j\frac{2\pi}{\lambda}\Delta_{y,z}w} \\ -w \end{bmatrix} \stackrel{\text{def}}{=} \acute{\mathbf{q}}_z.$$

As a result,

$$\hat{u} = \text{Re}\left\{ -[\acute{\mathbf{q}}_z]_1 \, e^{j\frac{2\pi}{\lambda}(\Delta_{x,y}+\Delta_{y,z})\hat{w}} \right\}$$
$$\hat{v} = \text{Re}\left\{ -[\acute{\mathbf{q}}_z]_2 \, e^{j\frac{2\pi}{\lambda}\Delta_{y,z}\hat{w}} \right\}$$
$$\hat{w}_{\text{coarse}} = -[\acute{\mathbf{q}}_z]_3$$
$$\hat{\phi} = \begin{cases} \arctan\left\{\frac{\hat{v}}{\hat{u}}\right\} & \text{if } \hat{u} \geq 0 \\ \arctan\left\{\frac{\hat{v}}{\hat{u}}\right\} + \pi & \text{if } \hat{u} < 0 \end{cases}$$
$$\hat{\theta} = \arccos\{\hat{w}\}$$

with $\hat{w}_{\text{fine},1}$ remains as in (15), $\hat{w}_{\text{fine},2}$ as in (16), and $\hat{w}$ as in (17).

D. If the Two Array-Axes Are Arbitrarily Oriented

In the general case that the two parallel array-axes are arbitrarily oriented, a new coordinates (x', y', z') could be defined such that the two array-axes would fit with one of the special cases in Sections III-A–III-C. In reference to these (x', y', z'), the directional cosines (u', v', w') are estimated. Then the following rotational transformation through the Euler angles (α, β, τ) (see [1, Fig. 3 and p. 147]) would give the Cartesian directional cosines $(\hat{u}, \hat{v}, \hat{w})$ in the Cartesian coordinates (x, y, z).

$$\begin{bmatrix} u \\ v \\ w \end{bmatrix} = \begin{bmatrix} \cos\tau & \sin\tau & 0 \\ -\sin\tau & \cos\tau & 0 \\ 0 & 0 & 1 \end{bmatrix} \begin{bmatrix} 1 & 0 & 0 \\ 0 & \cos\beta & \sin\beta \\ 0 & -\sin\beta & \cos\beta \end{bmatrix} \begin{bmatrix} \cos\alpha & \sin\alpha & 0 \\ -\sin\alpha & \cos\alpha & 0 \\ 0 & 0 & 1 \end{bmatrix} \begin{bmatrix} u' \\ v' \\ w' \end{bmatrix}.$$

IV. A Full Algorithm to Illustrate How to Apply the New Technique in Section III

The new "vector-cross-product" direction-finding technique proposed in Section III may be applied to *any* eigen-based parameter-estimation algorithm that can estimate a source's steering vector (to at least within a possibly unknown complex-value scalar).

To illustrate how so, this section will consider the "uni-vector-sensor ESPRIT" algorithm of [6], which is originally developed for an electromagnetic vector-sensor of *collocated* component-antennas. This section will instead show how the technique in Section III can modify [6] for a *spatially spread* vector-sensor as defined in the boxed description in Section II.

A. Review of Data Model and Algorithm of [6] for a Collocated Electromagnetic Vector-Sensor

Multiple completely polarized transverse electromagnetic waves, having traveled through an homogeneous isotropic medium, impinge upon a single electromagnetic vector-sensor, with spatially *collocated* component-antennas, all at the origin of the Cartesian coordinates. The kth such wavefront is associated with the steering vector $\mathbf{a}_k$, defined analogously as in (1). Let the kth incoming signal $s_k(t)$ to have power $\mathcal{P}_k$, but to be temporally monochromatic at a frequency f_k (distinct from all other incident sources' frequencies) with an initial phase of ϵ_k. With K such incident sources, the 6×1 data-vector collected at time t equals $\mathbf{z}(t) = \sum_{k=1}^{K} \sqrt{\mathcal{P}_k}\mathbf{a}_k e^{j2\pi f_k t + \epsilon_k} + \mathbf{n}(t)$, where $\mathbf{n}(t)$ symbolizes the additive noise at the electromagnetic vector-sensor.[8]

The *Uni-Vector-Sensor ESPRIT* algorithm [6] would form these two time-delayed data-subsets out of the aforementioned collected data: $\{\mathbf{z}(t_n), \forall n = 1, \ldots, N\}$ and $\{\mathbf{z}(t_n + \Delta_T), \forall n = 1, \ldots, N\}$, where Δ_T represents a constant time-delay between the two sets of time samples.

The following will summarize the algorithmic steps of the *Uni-Vector-Sensor ESPRIT* algorithm. For the motivations underlying these algorithmic steps, please refer to the lengthy exposition in [6] itself.

{1.} Form the $6 \times N$ data-matrices $\mathbf{Z}_1 = [\mathbf{z}(t_1), \mathbf{z}(t_2), \ldots, \mathbf{z}(t_N)]$ and $\mathbf{Z}_2 = [\mathbf{z}(t_1 + \Delta_T), \mathbf{z}(t_2 + \Delta_T), \ldots, \mathbf{z}(t_N + \Delta_T)]$.[9] Then, form the 6×6 data-correlation matrices $\mathbf{R}_1 = \mathbf{Z}_1\mathbf{Z}_1^H$ and $\mathbf{R}_2 = \mathbf{Z}_2\mathbf{Z}_2^H$, where the superscript ^{H} denotes the Hermitian operator.

{2.} Apply ESPRIT to the matrix-pencil $\{\mathbf{R}_1, \mathbf{R}_2\}$, as follows, to estimate all K impinging sources' steering-vectors:

{2a.} Let $\mathbf{E}_1$ denote the $6 \times K$ signal-subspace eigenvector matrix whose K columns are the 6×1 signal-subspace eigenvectors associated with the K largest eigenvalues of $\mathbf{R}_1$. Let $\mathbf{E}_2$ denote the corresponding signal-subspace eigenvector matrix for $\mathbf{R}_2$.

{2b.} Define the $K \times K$ matrix

$$\mathbf{\Psi} = \left(\mathbf{E}_1^H\mathbf{E}_1\right)^{-1}\left(\mathbf{E}_1^H\mathbf{E}_1\right) = \mathbf{T}^{-1}\mathbf{\Phi}\mathbf{T}$$

[8]The technique proposed in Section III may be readily applied to other data models, and not restricted to the one reviewed here of [6]. This present data model serves only as an illustrative example.

[9]The two datasets $\mathbf{Z}_1$ and $\mathbf{Z}_2$ are interrelated by the temporal "invariances" of $\{e^{j(2\pi f_k \Delta_T), k=1,2,\ldots,K}\}$, thereby allowing the use of the parameter-estimation method of Estimation of Signal Parameters Via Rotational Invariance Techniques ("ESPRIT") [2].

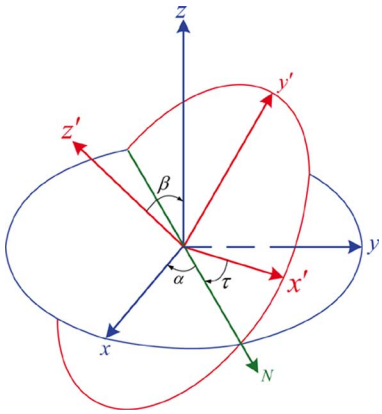

Fig. 3. The Cartesian coordinates (x', y', z') are rotated through the Euler angles (α, β, τ), to give a second set of Cartesian coordinates (x, y, z). (This diagram is based on a similar diagram in Wikipedia's entry on "Euler angles".)

where the jth eigenvalue of $\mathbf{\Psi}$ equals $\{[\mathbf{\Phi}]_{j,j} = e^{j2\pi f_j \triangle_T}, j = 1, \ldots, K\}$ and the corresponding right-eigenvector constitutes the jth column of $\mathbf{T}$.

{2c.} The K impinging sources' steering-vectors of (1) may be estimated, to within a complex-value multiplicative scalar, as

$$[\hat{\mathbf{a}}_1, \ldots, \hat{\mathbf{a}}_K] = \frac{1}{2}\{\mathbf{E}_1\mathbf{T}^{-1} + \mathbf{E}_2\mathbf{T}^{-1}\mathbf{\Phi}^{-1}\}.$$

These K *unknown* complex-value multiplicative scalars arise from the eigen-decomposition of $\mathbf{\Psi}$.

{3.} Apply the vector-cross-product of (2) to the kth source's above-estimated steering-vectors, as follows, to obtain the three corresponding Cartesian direction-cosine estimates:

$$\begin{bmatrix} \hat{u}_k \\ \hat{v}_k \\ \hat{w}_k \end{bmatrix} = \frac{\hat{\mathbf{e}}_k}{\|\hat{\mathbf{e}}_k\|} \times \frac{\hat{\mathbf{h}}_k^*}{\|\hat{\mathbf{h}}_k\|}.$$

The kth source's azimuth-elevation direction-of-arrival can then be estimated as

$$\hat{\theta}_k = \arcsin(\sqrt{\hat{u}_k^2 + \hat{v}_k^2}) = \arccos(\hat{w}_k),$$
$$\hat{\phi}_k = \arctan(\hat{v}_k/\hat{u}_k)$$

and the corresponding polarization parameters can then be estimated as

$$\hat{\gamma}_k = \arctan\frac{\hat{g}_{k,1}}{\hat{g}_{k,2}}, \quad (18)$$
$$\hat{\eta}_k = \angle\hat{g}_{k,1} \quad (19)$$

where

$$\hat{\mathbf{g}}_k = \begin{bmatrix} \hat{g}_{k,1} \\ \hat{g}_{k,2} \end{bmatrix} = \left[\mathbf{\Theta}^H(\hat{\theta}_k, \hat{\phi}_k)\mathbf{\Theta}(\hat{\theta}_k, \hat{\phi}_k)\right]^{-1}\mathbf{\Theta}^H(\hat{\theta}_k, \hat{\phi}_k)\hat{\mathbf{a}}_k. \quad (20)$$

B. Applying Section III's Proposed Method, to the Uni-Vector-Sensor ESPRIT Algorithm of [6], But Now With the Component-Antennas Spatially Spread as in Section II

Suppose now the *spatially spread* electromagnetic vector-sensor of Section II is now deployed, instead of a *spatially collocated* electromagnetic vector-sensor.

The 6×1 data-vector collected at time t would now equal $\tilde{\mathbf{z}}(t) = \sum_{k=1}^{K}\sqrt{\mathcal{P}_k}\tilde{\mathbf{a}}_k e^{j2\pi f_k t + \epsilon_k} + \mathbf{n}(t)$, instead. From this, Section IV-A's algorithmic steps $\{1.\}, \{2a.\}, \{2b.\}$, and $\{2c.\}$ can still follow here, but now with a tilde atop all symbols.

However, as for $\hat{u}_k, \hat{v}_k, \hat{w}_k, \hat{\phi}_k, \hat{\theta}_k$ of the preceding Section IV-A, replace them by their counterpart estimation-formulas newly defined in Sections III-A–1, III-A–2, III-B–1, III-B–2, III-C–1, or III-C–2.[10]

V. Monte Carlo Simulation for the Algorithm Obtained From Modifying [6] by the Technique Proposed in Section III

The proposed scheme's direction-finding efficacy and extended-aperture capability are demonstrated by Monte Carlo simulations.

Fig. 4 shows a two-source scenario, whereas Fig. 5 shows a three-source scenario.[11] Each graph plots the composite mean-square-error of each incident source's three Cartesian direction-cosine estimates, versus the inter-antenna spacing parameter $\Delta/\lambda = \ell$. Each data-point on each graph consists of 1000 statistically independent Monte Carlo trials. These estimate uses 400 temporal snapshots. All sources have unity power. Each source's signal-to-noise ratio equals 30 dB. The "spatially spread" electromagnetic vector-sensor conforms to a rectangular grid and lies at some nonzero angle to all three Cartesian axes. Specifically, referring to the array geometric symbols defined in Fig. 2: $(\tilde{\theta}, \tilde{\phi}) = (45°, 45°)$, $(x_h, y_h, z_h) = \ell\lambda(2, 1, \sqrt{2})$, $\Delta/\lambda = \Delta_{x,y}/\lambda = \Delta_{y,z}/\lambda = \ell$, with λ defined to equal the minimum of $\lambda_1, \ldots, \lambda_K$.

Figs. 4 and 5 clearly demonstrate the proposed scheme's success in resolving the incident sources, even if the electromagnetic vector-sensor's six component-antennas are spaced very far apart. In fact, this spatial *non*-collocation leads to orders-of-magnitude improvement in estimation accuracy, even as mutual coupling is reduced. Moreover, the estimation is very close to the Cramér-Rao lower bound (derived in the Appendix) as the inter-antenna spacing increases above a few wavelengths.

VI. Conclusion

Many direction-finding advantages are offered by the recent synergy between interferometry and "vector cross-product" Poynting-vector estimation. However, the practicality of this synergy is limited by the mutual coupling across the six component-antennas comprising the electromagnetic vector-sensor. To alleviate this mutual-coupling problem, and thus to simplify the antenna implementation and to reduce hardware cost, this paper show a way how to achieve "vector cross-product"

[10]For polarization estimation, (18)–(20) remain applicable, except that (20) needs to have its $\hat{\mathbf{a}}_k$ replaced by $\hat{\tilde{\mathbf{a}}}_k$, and to have its $\mathbf{\Theta}(\hat{\theta}_k, \hat{\phi}_k)$ replaced by $\mathbf{d}(\hat{\theta}_k, \hat{\phi}_k)\mathbf{\Theta}(\hat{\theta}_k, \hat{\phi}_k)$.

[11]The estimation bias is about an order-of-magnitude smaller than the corresponding estimation standard deviation.

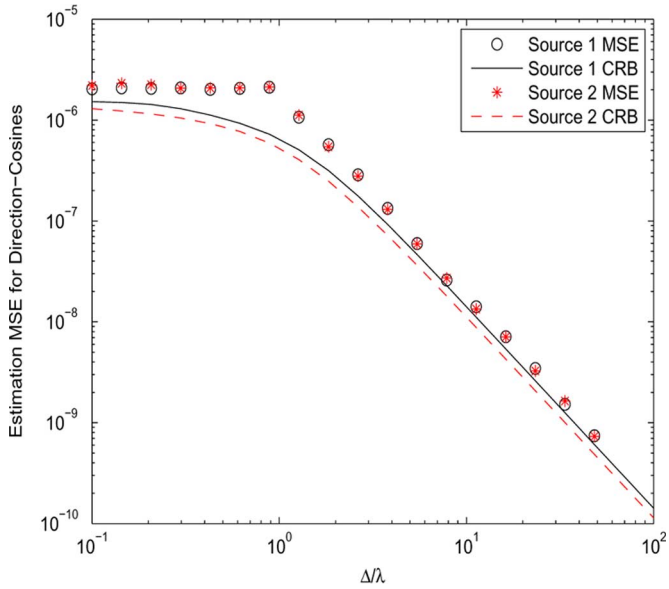

Fig. 4. The composite mean-square-error of the Cartesian direction-cosines estimates, for *two* incident sources, at digital frequencies $f_1' = 0.1$ and $f_2' = 0.1265$, respectively, with $(\theta_1, \phi_1, \gamma_1, \eta_1) = (56°, 55°, 45°, -90°)$ and $(\theta_2, \phi_2, \gamma_2, \eta_2) = (54°, 57°, 45°, 90°)$.

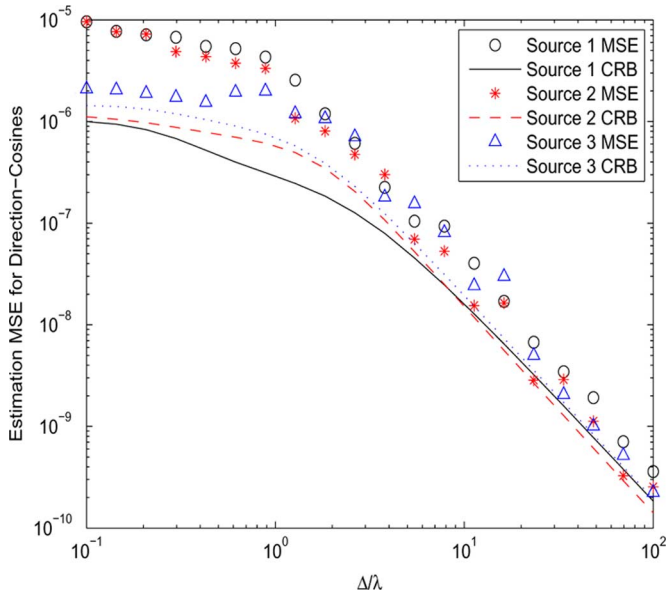

Fig. 5. The composite mean-square-error of the Cartesian direction-cosines estimates, for *three* incident sources, at digital frequencies $f_1' = 0.1$, $f_2' = 0.1265$, and $f_3' = 0.1165$, respectively, with $(\theta_1, \phi_1, \gamma_1, \eta_1) = (35°, 42°, 45°, -90°)$, $(\theta_2, \phi_2, \gamma_2, \eta_2) = (43°, 35°, 45°, 90°)$, and $(\theta_3, \phi_3, \gamma_3, \eta_3) = (52°, 52°, 45°, -90°)$. The same "spatially spread" electromagnetic vector-sensor configuration is used here as in Fig. 4.

Poynting-vector estimation while spacing the six component-antennas far from each other. This spatial noncollocation extends the spatial aperture, to improve direction-finding accuracy by *orders of magnitude*, at *lower* hardware cost.

APPENDIX
DERIVATION OF THE CRAMÉR-RAO BOUND

To avoid unnecessary distraction, simple assumptions will be made of the signal statistical model in Section IV-A: One single pure-tone's frequency and known initial phase are presumed as known constants. The data sampling instants occur at $t = nT_s$, where T_s refers to the time-sampling period, and $\mathbf{n}(t)$ denotes a 6×1 vector of additive zero-mean spatio-temporally uncorrelated Gaussian noise, with an unknown covariance-matrix of $\mathbf{\Gamma}_0$, which is deterministic, 6×6, diagonal with all diagonal elements equal to σ^2, which represents the known noise-variance at each component-antenna.

With N number of time-samples, the data-set is $6 \times N$ and equals

$$\begin{aligned}\boldsymbol{\zeta} &= [(\mathbf{z}(T_s))^T, \ldots, (\mathbf{z}(NT_s))^T]^T \\ &= \underbrace{\sum_{k=1}^{K} (\mathbf{s}_k \otimes \tilde{\mathbf{a}}_k)}_{=\boldsymbol{\mu}} + \underbrace{[(\mathbf{n}(T_s))^T, \ldots, (\mathbf{n}(NT_s))^T]^T}_{=\boldsymbol{\nu}},\end{aligned}$$

where $\mathbf{s}_k = e^{j\epsilon}[e^{j2\pi f_k T_s}, e^{j4\pi f_k T_s}, \ldots, e^{j2N\pi f_k T_s}]^T$, $\otimes$ symbolizes the Kronecker product, $\boldsymbol{\nu}$ represents a $6N \times 1$ noise vector with a spatio-temporal covariance matrix of $\mathbf{\Gamma} = \mathbf{I}_N \otimes \mathbf{\Gamma}_0$, and $\mathbf{I}_N$ denotes an $N \times N$ identity matrix. Therefore, $\boldsymbol{\zeta} \sim \mathcal{N}(\boldsymbol{\mu}, \mathbf{\Gamma})$, i.e., a Gaussian vector with mean $\boldsymbol{\mu}$ and covariance $\mathbf{\Gamma}$.

Collect all deterministic unknown entities into a $4K \times 1$ vector, $\boldsymbol{\psi} = [\theta_1, \phi_1, \gamma_1, \eta_1, \ldots, \theta_K, \phi_K, \gamma_K, \eta_K]^T$. The resulting $4K \times 4K$ Fisher Information Matrix (FIM), $\mathbf{J}$, would have its (i, j)th entry equal to [18, eq. (8.34)])

$$\begin{aligned}[\mathbf{J}]_{i,j} = 2\mathrm{Re}\left[\left(\frac{\partial \boldsymbol{\mu}}{\partial [\boldsymbol{\psi}]_i}\right)^H \mathbf{\Gamma}^{-1} \left(\frac{\partial \boldsymbol{\mu}}{\partial [\boldsymbol{\psi}]_j}\right)\right] \\ + \mathrm{Tr}\left[\mathbf{\Gamma}^{-1} \frac{\partial \mathbf{\Gamma}}{\partial [\boldsymbol{\psi}]_i} \mathbf{\Gamma}^{-1} \frac{\partial \mathbf{\Gamma}}{\partial [\boldsymbol{\psi}]_j}\right]\end{aligned}$$

where $\mathrm{Re}[\cdot]$ denotes the real-value part of the entity inside $[\cdot]$, and $\mathrm{Tr}[\cdot]$ represents the trace operator.

Any unbiased estimation of the directions-of-arrival would have these Cramér-Rao lower bounds

$$\begin{aligned}\mathrm{CRB}(\theta_k) &= \left[\mathbf{J}^{-1}\right]_{4k-3,4k-3} \\ \mathrm{CRB}(\phi_k) &= \left[\mathbf{J}^{-1}\right]_{4k-2,4k-2}.\end{aligned}$$

These equations may be easily evaluated by MATLAB's symbolic toolbox, to obtain the Cramér-Rao bound curves in Figs. 4 and 5.

For a general K-source scenario, the Fisher Information Matrix would be $4K \times 4K$ in size, to be specified by $8K^2 + 2K$ number of distinct scalar equations (after accounting for symmetry in the matrix). As illustration the following equations present the 10 equations for the Fisher Information Matrix's 16 elements in the single-source case, for the specific case of $\Delta_{x,y} = \Delta_{y,z} = k\lambda$. The equations would become excessively lengthy to state here for the general array manifold of (3). Define the elements of the single-source Fisher Information Matrix as follows:

$$\mathbf{J} = \begin{bmatrix} J_{\theta,\theta} & J_{\theta,\phi} & J_{\theta,\gamma} & J_{\theta,\eta} \\ J_{\phi,\theta} & J_{\phi,\phi} & J_{\phi,\gamma} & J_{\phi,\eta} \\ J_{\gamma,\theta} & J_{\gamma,\phi} & J_{\gamma,\gamma} & J_{\gamma,\eta} \\ J_{\eta,\theta} & J_{\eta,\phi} & J_{\eta,\gamma} & J_{\eta,\eta} \end{bmatrix}$$

Using symbolic programming by MATLAB and Mathematica

$$
\begin{aligned}
J_{\theta,\theta} = \frac{2N}{\sigma^2\lambda^2}\{&\lambda^2 + 4\pi^2 z_h^2 - 8k\lambda\pi^2 z_h(\cos\phi)c_1 \\
&+ 16k^2\lambda^2\pi^2(\cos\tilde{\theta})^2 + 4k^2\lambda^2\pi^2 c_1^2 \\
&+ 8k\lambda\pi^2(\cos\gamma)^2[(\cos\tilde{\theta})(-2z_h + z_h(\cos\phi)^2 \\
&+ x_h(\cos\phi)\sin(2\gamma) + y_h(\sin\phi)\sin(2\gamma)) \\
&+ z_h\cos(\phi-\tilde{\phi})\sin(2\gamma)(\sin\tilde{\theta})] \\
&+ 4k\lambda\pi^2(\cos\theta)^4\Big[-3k\lambda\sin(2\phi)c_3c_2 \\
&+ (\cos\gamma)^2(-2z_h(\cos\tilde{\theta}) + (y_h(\cos\tilde{\phi})\sin(2\phi) \\
&+ (2y_h + x_h\sin(2\phi))(\sin\tilde{\phi}))(\sin\tilde{\theta})) \\
&+ 3k\lambda\left(-1 + 2(\cos\tilde{\theta})^2 + c_2^2\right) \\
&+ (\cos\phi)^3(\sin\phi)(k\lambda(\cos\tilde{\theta})^2 \\
&\times \sin(2\tilde{\phi}) + 2x_h(\cos\gamma)^2 c_3 \\
&+ (\cos\tilde{\phi})(-2k\lambda(\sin\tilde{\phi}) + 2y_h(\cos\gamma)^2(\sin\tilde{\theta}))) \\
&+ (\cos\phi)^4\Big(-k\lambda(\cos\tilde{\theta})^2 + 2(\cos\gamma)^2(x_h(\cos\tilde{\phi}) \\
&- y_h(\sin\tilde{\phi}))(\sin\tilde{\theta}) + k\lambda\left(1 - 2c_2^2\right)\Big) \\
&- (\cos\phi)^2\Big(2(\cos\gamma)^2(z_h(\cos\tilde{\theta}) - x_h c_2) \\
&+ k\lambda\left(-2 + (\cos\tilde{\theta})^2 + 5c_2^2\right)\Big)\Big] \\
&- 4\pi^2\cos\theta[-2c_{10}k\lambda z_h(\cos\tilde{\theta})\sin(2\phi) \\
&+ 2(\sin\theta)(x_h z_h(\cos\phi) + y_h z_h(\sin\phi) \\
&+ k\lambda(\cos\phi)^3(-z_h c_2(\sin\gamma)^2 \\
&+ (\cos\tilde{\theta})(-x_h(\sin\gamma)^2 + k\lambda c_2)) \\
&+ k\lambda(\cos\phi)^2\sin\phi(-z_h(\sin\gamma)^2 c_3 \\
&+ (\cos\tilde{\theta})(-y_h(\sin\gamma)^2 + k\lambda c_3)))] - 4\pi^2\cos\theta^2 \\
&\times\Big[-4k^2\lambda^2 - y_h^2 + z_h^2 + 11k^2\lambda^2(\cos\tilde{\theta})^2 \\
&- 2k^2\lambda^2\sin(2\phi)\sin(2\tilde{\phi}) \\
&+ 2k^2\lambda^2(\cos\tilde{\theta})^2\sin(2\phi)\sin(2\tilde{\phi}) + 4k^2\lambda^2 c_2^2 \\
&+ 2k\lambda\cos\gamma^2(-3z_h(\cos\tilde{\theta}) \\
&+ (y_h(\cos\tilde{\phi})\sin(2\phi) \\
&+ (2y_h + x_h\sin(2\phi))(\sin\tilde{\phi}))(\sin\tilde{\theta})) \\
&+ (\cos\phi)^2\left(3k^2\lambda^2 - x_h^2 + y_h^2\right. \\
&- k^2\lambda^2(\cos\tilde{\theta})^2 - 2k\lambda(\cos\tilde{\theta})(z_h - 2x_h c_{10}c_4) \\
&+ 4k\lambda z_h c_{10}c_2c_4 + 2k\lambda y_h c_3 \\
&+ 2k\lambda\cos\gamma^2(2x_h(\cos\tilde{\phi}) \\
&- 3y_h(\sin\tilde{\phi}))(\sin\tilde{\theta}) - 7k^2\lambda^2 c_2^2\Big) \\
&+ k\lambda(\cos\phi)^4(\sin\tilde{\theta}) \\
&\times(2x_h(\cos\tilde{\phi})(\sin\gamma)^2 - k\lambda(\cos\tilde{\phi})c_2 \\
&+ (\sin\tilde{\phi})(-2y_h(\sin\gamma)^2 + k\lambda c_3)) \\
&+ (\cos\phi)(-2x_h y_h(\sin\phi) + 4k\lambda c_{10} \\
&\times(\sin\theta)(y_h(\cos\tilde{\theta}) \\
&+ z_h c_3)) - 2k\lambda(\cos\phi)^3 \\
&\times(2c_{10}\sin\theta(y_h(\cos\tilde{\theta}) + z_h c_3) \\
&+ (\sin\phi)(\sin\tilde{\theta})(-x_h(\sin\gamma)^2(\sin\tilde{\phi}) \\
&+ (\cos\tilde{\phi})(-y_h(\sin\gamma)^2 + k\lambda c_3)))\Big] \\
&- 8k^2\lambda^2\pi^2(\cos\phi)(\cos\tilde{\phi})\sin(2\gamma)[\sin(2\tilde{\theta})] \\
&- 8k^2\lambda^2\pi^2(\sin\phi)\sin(2\gamma)(\sin\tilde{\phi})[\sin(2\tilde{\theta})] \\
&+ 4k\lambda\pi^2(\cos\theta)^3[c_{10}\sin(2\phi)(-2z_h(\cos\tilde{\theta}) \\
&+ 2\cos(\phi-\tilde{\phi})(x_h(\cos\phi) \\
&+ y_h(\sin\phi))(\sin\tilde{\theta})) \\
&- (\sin\theta)((\cos\gamma)^2(3 + \cos(2\phi)) \\
&\times(\cos\phi(x_h(\cos\tilde{\theta}) + z_h c_2) \\
&+ (\sin\phi)(y_h(\cos\tilde{\theta}) + z_h c_3)) \\
&- 0.5k\lambda(7 + \cos(2\phi))\cos(\phi-\tilde{\phi})(\sin(2\tilde{\theta})))]\Big\}
\end{aligned}
$$

$$
\begin{aligned}
J_{\theta,\phi} &= J_{\phi,\theta} \\
&= \frac{N}{2\sigma^2\lambda^2}\pi\{16k\lambda\pi(\cos\phi)^4\sin(2\theta)(\sin\tilde{\theta}) \\
&\times[(-x_h + x_h(\cos\gamma)^2(1 + (\cos\theta)^2) \\
&- 2c_{10}y_h(\cos\theta))(\sin\tilde{\phi}) \\
&+ (\cos\tilde{\phi})(-y_h + y_h(\cos\gamma)^2(1 + (\cos\theta)^2) \\
&+ 2c_{10}x_h(\cos\theta) + k\lambda(\sin\theta)^2 c_3)] \\
&+ 8k\lambda\pi(\cos\phi)^3[2k\lambda(\cos\theta)\cos(2\tilde{\phi}) \\
&\times(\cos\tilde{\theta})^2(\sin\phi)(\sin\theta)^3 \\
&+ k\lambda(\sin\phi)\sin(2\theta) \\
&+ 2x_h(\sin\phi)\sin(2\theta)c_2 + 2z_h c_3 - 2z_h(\cos\gamma)^2 c_3 \\
&+ (\cos\theta)^4(z_h + z_h\cos(2\gamma) - 2k\lambda(\cos\tilde{\theta}))c_3 \\
&+ 2y_h(\cos\gamma)^2(\sin\phi)\sin(2\theta)c_3 \\
&+ 2(\cos\theta)^2(-z_h(\sin\tilde{\phi}) \\
&+ 4c_{10}c_4(y_h(\cos\tilde{\phi}) + x_h(\sin\tilde{\phi})))(\sin\tilde{\theta}) \\
&- 4(\cos\theta)(k\lambda(\cos\tilde{\phi})^2(\sin\phi)(\sin\theta) \\
&+ (\cos\gamma)(\cos\tilde{\phi})(z_h(\cos\eta)(\sin\gamma) \\
&+ x_h(\cos\gamma)c_4)(\sin\tilde{\theta}) + y_h c_4 c_3) \\
&+ 2(\cos\tilde{\theta})(y_h + y_h(\cos\gamma)^2 \\
&\times(-1 + (\cos\theta)^4) - 2c_{10}x_h(\cos\theta) \\
&+ 2c_{10}x_h(\cos\theta)^3 - (\cos\theta)^2(y_h - 2k\lambda c_3)) \\
&+ 2(\cos\theta)^3(2z_h 2c_{10}c_2 + c_4(-k\lambda + 2k\lambda(\cos\tilde{\phi})^2 \\
&- 2x_h(\cos\gamma)^2 c_2 + 2y_h(\cos\gamma)^2 c_2)) - k\lambda c_6] \\
&+ 8(\cos\phi)[-2k\lambda\pi(\cos\theta)^3(2x_h(\cos\gamma)^2 c_2 c_4 \\
&+ 2c_{10}(x_h(\cos\tilde{\theta}) + z_h c_2)) \\
&+ 2k\lambda\pi(\cos\theta)^4(-3k\lambda(\cos\tilde{\theta})c_3 \\
&+ (\cos\gamma)^2(y_h(\cos\tilde{\theta}) + z_h c_3)) \\
&- 2\pi(y_h z_h + 4k^2\lambda^2(\cos\tilde{\theta})c_3 \\
&- 2k\lambda(\cos\gamma)^2(y_h(\cos\tilde{\theta}) + z_h c_3)) \\
&+ 2k\lambda\pi(\cos\theta)(2c_{10}(x_h(\cos\tilde{\theta}) + z_h c_3) \\
&- 4c_4(k\lambda(\cos\tilde{\theta})^2 \\
&+ y_h(\cos\gamma)^2 c_3)) + (\cos\theta)^2(2\pi y_h z_h - \lambda x_h c_{11} \\
&- 6k\lambda\pi(\cos\gamma)^2(y_h(\cos\tilde{\theta}) + z_h c_3) \\
&+ 7k^2\lambda^2\pi c_6)] \\
&- 4\left[2k\lambda\pi(\cos\theta)^2(\sin\theta)\right. \\
&\times(\sin\tilde{\theta})(2c_{10}\sin(2\phi)(y_h(\cos\tilde{\phi})
\end{aligned}
$$

$$
\begin{aligned}
&+ x_h(\sin\tilde{\phi})) + 2(\cos\gamma)^2(\cos\theta)(y_h(\cos\tilde{\phi})\\
&+ (x_h - y_h\sin(2\phi))(\sin\tilde{\phi}))\\
&- 3k\lambda(\cos\theta)(\cos(2\tilde{\phi})\sin(2\phi)\\
&+ \sin(2\tilde{\phi}))(\sin\tilde{\theta})) + \sin(2\theta)\,(-\lambda z_h c_{11}\\
&+ \pi\left(2x_h y_h - 4k\lambda(\cos\gamma)^2(y_h(\cos\tilde{\phi})\right.\\
&+ x_h(\sin\tilde{\phi}))(\sin\tilde{\theta})\\
&+ 4k^2\lambda^2\sin(2\tilde{\phi})(\sin\tilde{\theta})^2 + \sin(2\phi)\\
&\times\left(-4k^2\lambda^2 + x_h^2 - y_h^2\right.\\
&-\ \left.\left.4k\lambda x_h(\cos\gamma)^2 c_2 + 8k^2\lambda^2 c_2^2\right)\right))\\
&+ 2(\sin\phi)(k\lambda\pi(\cos\theta)^4\\
&\times(2(\cos\gamma)^2(x_h(\cos\tilde{\theta}) + z_h c_2) - 3k\lambda c_5)\\
&- 2\pi(x_h z_h - 2k\lambda(\cos\gamma)^2(x_h(\cos\tilde{\theta})\\
&+ z_h c_2) + 2k^2\lambda^2 c_5) + (\cos\theta)^2(2\pi x_h z_h + \lambda y_h c_{11}\\
&- 6k\lambda\pi(\cos\gamma)^2(x_h(\cos\tilde{\theta}) + z_h c_2)\\
&+ 7k^2\lambda^2\pi c_5))\big]\\
&+ \pi(\cos\phi)^2\left[-16k\lambda z_h(\cos\gamma)^2(\cos\theta)^4(\sin\phi)c_2\right.\\
&+ 32(\cos\theta)(x_h y_h(\sin\theta)\\
&- k\lambda y_h(\cos\tilde{\theta})c_{10}c_4(\sin\theta)\\
&- k\lambda z_h c_{10}(\sin\phi)c_3)\\
&+ 16k\lambda(\cos\theta)^2(x_h(\cos\gamma)^2(\cos\tilde{\theta})c_4(\sin\theta)\\
&+ z_h(\sin\phi)c_2 - 4c_{10}(\sin\theta)(x_h(\cos\tilde{\phi})\\
&- y_h(\sin\tilde{\phi}))(\sin\tilde{\theta}))\\
&- 8k\lambda(\cos\theta)^3(-4z_h 4c_{10}(\sin\phi)c_3\\
&+ (\sin\theta)(5k\lambda\sin(2\tilde{\phi}) - 2(\cos\gamma)^2(y_h(\cos\tilde{\phi})\\
&+ x_h(\sin\tilde{\phi}))(\sin\tilde{\theta})))\\
&- k\lambda(16x_h(\cos\tilde{\theta})(\sin\gamma)^2 c_4(\sin\theta)\\
&+ k\lambda(\cos\tilde{\theta})^2(18\sin(2\theta) - 5\sin(4\theta))\sin(2\tilde{\phi})\\
&+ 4(\sin(2\theta)(-7k\lambda\sin(2\tilde{\phi})\\
&+ (3 + 5\cos(2\gamma))(y_h(\cos\tilde{\phi})\\
&+ x_h(\sin\tilde{\phi}))(\sin\tilde{\theta}))\\
&+ 2(\cos\tilde{\phi})(\sin\phi)(2z_h(\sin\gamma)^2(\sin\tilde{\theta})\\
&-\ \left.k\lambda(\sin\theta)^4\sin(2\tilde{\theta}))))\right]\Big\}
\end{aligned}
$$

$$
\begin{aligned}
J_{\theta,\gamma} &= J_{\gamma,\theta}\\
&= \frac{N}{2\sigma^2}k\pi[(-6 + 6\cos(2\phi) + \cos(2(\phi-\theta))\\
&\quad + 6\cos(2\theta) + \cos(2(\phi+\theta)))\sin(2\gamma)\\
&\quad - 8(\cos\theta)(\sin\eta)\sin(2\phi)][-(\cos\tilde{\theta})(\sin\theta)\\
&\quad + (\cos\theta)\cos(\phi-\tilde{\phi})(\sin\tilde{\theta})],\\
J_{\theta,\eta} &= J_{\eta,\theta}\\
&= \frac{2N}{\sigma^2\lambda}2\pi(\sin\gamma)\{k\lambda(\cos\phi)^3(\cos\theta)\\
&\quad \times[(1 + (\cos\theta)^2)(\cos\tilde{\phi})(\sin\gamma)\\
&\quad + 2c_7(\sin\tilde{\phi})](\sin\tilde{\theta})\\
&\quad + k\lambda(\cos\phi)^2[-(1/4)(\cos\tilde{\theta})\\
&\quad \times(\sin\gamma)(5(\sin\theta) + \sin(3\theta))\\
&\quad + (\cos\theta)(\sin\phi)(-2c_7(\cos\tilde{\phi})\\
&\quad + (1 + (\cos\theta)^2)(\sin\gamma)c_3]\\
&\quad + (\sin\gamma)[-k\lambda(\cos\theta)^2(\cos\tilde{\theta})(\sin\theta)\\
&\quad + (z_h + 2k\lambda(\cos\tilde{\theta}))(\sin\theta)\\
&\quad + k\lambda(\cos\theta)^3(\sin\phi)(\sin\tilde{\phi})(\sin\tilde{\theta})\\
&\quad - (\cos\theta)(\sin\phi)(y_h + 2k\lambda c_3)]\\
&\quad + (\cos\phi)(\cos\theta)[-(\sin\gamma)(x_h\\
&\quad - 0.5k\lambda(-3 + \cos(2\theta))c_2)\\
&\quad + 2k\lambda(\cos\eta)(\cos\gamma)((\cos\tilde{\theta})c_4 - (\cos\theta)c_3)]\},\\
J_{\phi,\phi} &= \frac{2N}{\sigma^2\lambda^2}\left\{\lambda^2 + 4\pi^2x_h^2 + 16k^2\lambda^2\pi^2(\cos\tilde{\phi})^2\right.\\
&\quad - 16k^2\lambda^2\pi^2(\cos\tilde{\phi})^2(\cos\tilde{\theta})^2\\
&\quad - 8k^2\lambda^2\pi^2\sin(2\phi)\sin(2\tilde{\phi})\\
&\quad + 8k^2\lambda^2\pi^2(\cos\tilde{\theta})^2\sin(2\phi)\sin(2\tilde{\phi})\\
&\quad - 16k\lambda\pi^2x_h(\cos\gamma)^2(\cos\tilde{\phi})(\sin\tilde{\theta})\\
&\quad + 8k\lambda\pi^2y_h(\cos\gamma)^2(\cos\tilde{\phi})c_8\\
&\quad - 8k\lambda\pi^2x_h(\cos\theta)^3(\cos\tilde{\phi})c_{10}c_8\\
&\quad + 8k\lambda\pi^2x_h(\cos\gamma)^2(\sin\tilde{\phi})c_8\\
&\quad + 4\lambda\pi x_h(\cos\theta)\sin(2\gamma)[(\sin\eta)(\sin\phi)(\sin\theta)\\
&\quad + k\pi(\cos\eta)(\cos\tilde{\phi})\sin(2\phi)(\sin\tilde{\theta})]\\
&\quad - 2k\lambda\pi^2(\cos\theta)^4(\sin\tilde{\theta})(4x_h(\cos\gamma)^2(\cos\tilde{\phi})\\
&\quad + 3k\lambda(-2(\cos\tilde{\phi})^2\\
&\quad + \sin(2\phi)\sin(2\tilde{\phi}))(\sin\tilde{\theta}))\\
&\quad + (\cos\theta)^2\left(\lambda^2 - 4\pi^2x_h^2\right.\\
&\quad + \left.24k\lambda\pi^2x_h(\cos\gamma)^2c_2 - 28k^2\lambda^2\pi^2c_2^2\right)\\
&\quad + k\lambda\pi^2(\cos\phi)^3(\sin\phi)(\sin\tilde{\theta})[8x_h(\cos\gamma)^2\\
&\quad \times(\cos\theta)^4(\sin\tilde{\phi}) + 8x_h(\sin\gamma)^2(\sin\tilde{\phi})\\
&\quad - 16c_{10}y_h(\cos\theta)^3(\sin\tilde{\phi})\\
&\quad + 16c_{10}(\cos\theta)(-x_h c_9 + y_h(\sin\tilde{\phi}))\\
&\quad - (\cos\tilde{\phi})(-8y_h(\sin\gamma)^2(\sin\theta)^2\\
&\quad + k\lambda(11 + 4\cos(2\theta) + \cos(4\theta))c_3)\\
&\quad - 8(\cos\theta)^2(y_h(\cos\gamma)^2c_9\\
&\quad + (\sin\tilde{\phi})(x_h - 2k\lambda c_2))]\\
&\quad - 4k\lambda\pi^2(\cos\phi)^4(\sin\theta)^2\left[-k\lambda + k\lambda(\cos\tilde{\theta})^2\right.\\
&\quad - 2x_h(\sin\gamma)^2c_2 + 2y_h c_3 - 2y_h(\cos\gamma)^2c_3\\
&\quad - 4c_{10}(\cos\theta)(y_h(\cos\tilde{\phi})\\
&\quad + x_h(\sin\tilde{\phi}))(\sin\tilde{\theta}) + 2k\lambda c_2^2\\
&\quad + (\cos\theta)^2\left(-k\lambda(\cos\tilde{\theta})^2 + 2(\cos\gamma)^2\right.\\
&\quad \times\ \left.(x_h c_2 - y_h c_3) + k\lambda\left(1 - 2c_2^2\right)\right)]\\
&\quad - 4\pi^2(\cos\phi)^2(\sin\theta)^2\left[-4k^2\lambda^2 + x_h^2 - y_h^2\right.\\
&\quad + 4k^2\lambda^2(\cos\tilde{\theta})^2 - k\lambda x_h(1 + 3\cos(2\gamma))c_2\\
&\quad + 4k\lambda y_h(\cos\gamma)^2c_3 + 4c_{10}k\lambda\\
&\quad \times(\cos\theta)(y_h c_2 + x_h c_3) + 7k^2\lambda^2c_2^2 - k\lambda(\cos\theta)^2\\
&\quad \times\left(3k\lambda(\cos\tilde{\theta})^2 + 2y_h(\cos\gamma)^2c_3\right.\\
&\quad +\ \left.\left.k\lambda\left(-3 + 5c_2^2\right)\right)\right] + 8\pi(\cos\phi)\\
&\quad \times[-0.5c_{11}\lambda y_h(\cos\theta)(\sin\theta) + \pi(\sin\phi)(-x_h y_h\\
&\quad + k\lambda(\cos\gamma)^2(\cos\theta)^4(y_h(\cos\tilde{\phi})\\
&\quad + x_h(\sin\tilde{\phi}))(\sin\tilde{\theta})
\end{aligned}
$$

$$\mathrm{CRB}_c(\theta) = \frac{\sigma^2}{2N}$$

$$\mathrm{CRB}_c(\phi) = \frac{\sigma^2}{2N}\frac{1}{\{1+(\cos\theta)^2[1-2(\cos\eta)^2-2(\cos\gamma)^2(\sin\eta)^2]\}}$$

$$\mathrm{CRB}_c(\gamma) = \frac{\sigma^2}{4N}\frac{[1+(\cos\theta)^2-2(\cos\theta)^2(\cos\gamma)^2(\sin\eta)^2]}{\{1+(\cos\theta)^2[1-2(\cos\eta)^2-2(\cos\gamma)^2(\sin\eta)^2]\}}$$

$$\mathrm{CRB}_c(\eta) = \frac{\sigma^2}{4N}\frac{1}{(\sin\gamma)^2}\frac{[1+(\cos\theta)^2-2(\cos\theta)^2(\cos\eta)^2]}{\{1+(\cos\theta)^2[1-2(\cos\eta)^2-2(\cos\gamma)^2(\sin\eta)^2]\}}$$

$$\begin{aligned}
&+(\cos\theta)^2(x_h y_h - 3k\lambda(\cos\gamma)^2(y_h(\cos\tilde{\phi})\\
&+x_h(\sin\tilde{\phi}))(\sin\tilde{\theta}) + 7k^2\lambda^2(\cos\tilde{\phi})(\sin\tilde{\theta})c_3))]\Big\},\\
J_{\phi,\gamma} &= J_{\gamma,\phi}\\
&= \frac{-4N}{\sigma^2}(\cos\theta)\{\cos\eta - k\pi(\sin\eta)\\
&\times[\sin(2\phi)](\sin\theta)[\sin(\phi-\tilde{\phi})](\sin\tilde{\theta})\},\\
J_{\phi,\eta} &= J_{\eta,\phi}\\
&= \frac{2N}{\sigma^2\lambda}\pi(\sin\gamma)(\sin\theta)\{-2k\lambda(\cos\phi)^2(\sin\phi)\\
&\times[(1+(\cos\theta)^2)(\cos\tilde{\phi})(\sin\gamma)\\
&+2c_7(\sin\tilde{\phi})](\sin\tilde{\theta})\\
&+2k\lambda(\cos\phi)^3[-2c_7(\cos\tilde{\phi})\\
&+(1+(\cos\theta)^2)(\sin\gamma)(\sin\tilde{\phi})]\\
&\times(\sin\tilde{\theta}) + (\sin\gamma)(\sin\phi)\\
&\times[2x_h - k\lambda(-3+\cos(2\theta))c_2]\\
&+(\cos\phi)[4k\lambda c_7 c_2 + (\sin\gamma)\\
&\times(-2y_h k\lambda(-3+\cos(2\theta))c_3)]\},\\
J_{\gamma,\gamma} &= \frac{4N}{\sigma^2}\\
J_{\gamma,\eta} &= J_{\eta,\gamma} = 0,\\
J_{\eta,\eta} &= \frac{4N(\sin\gamma)^2}{\sigma^2}
\end{aligned}$$

where

$$\begin{aligned}
c_1 &= (\cos\phi)(\cos\tilde{\theta})\\
c_2 &= (\cos\tilde{\phi})(\sin\tilde{\theta})\\
c_3 &= (\sin\tilde{\phi})(\sin\tilde{\theta})\\
c_4 &= (\sin\phi)(\sin\theta)\\
c_5 &= (\cos\tilde{\phi})\sin(2\tilde{\theta})\\
c_6 &= (\sin\tilde{\phi})\sin(2\tilde{\theta})\\
c_7 &= (\cos\eta)(\cos\gamma)(\cos\theta)\\
c_8 &= \sin(2\phi)(\sin\tilde{\theta})\\
c_9 &= (\cos\tilde{\phi})(\sin\theta)^2\\
c_{10} &= (\cos\eta)(\cos\gamma)(\sin\gamma)\\
c_{11} &= (\sin\eta)\sin(2\gamma).
\end{aligned}$$

The Cramér-Rao bounds would be excessively lengthy to state here for the spatially spread electromagnetic vector-sensor, even for the single-source case. These expressions are very long, because the Fisher Information matrix needs be inverted to produce the Cramér-Rao bounds. However, for $\ell = 0$ (i.e., the six component-antennas are spatially collocated), the Cramér-Rao bounds equal (see the equation at the top of the page).

REFERENCES

[1] H. Goldstein, *Classical Mechanics*, 2nd ed. Reading, MA: Addison-Wesley, 1980.

[2] R. Roy and T. Kailath, "ESPRIT—Estimation of signal parameters via rotational invariance techniques," *IEEE Trans. Acoust., Speech, Signal Process.*, vol. 37, no. 7, pp. 984–995, Jul. 1989.

[3] J. Li, "Direction and polarization estimation using arrays with small loops and short dipoles," *IEEE Trans. Antennas Propag.*, vol. 41, no. 3, pp. 379–387, Mar. 1993.

[4] A. Nehorai and E. Paldi, "Vector-sensor array processing for electromagnetic source localization," *IEEE Trans. Signal Process.*, vol. 42, no. 2, pp. 376–398, Feb. 1994.

[5] B. Hochwald and A. Nehorai, "Polarimetric modeling and parameter estimation with applications to remote sensing," *IEEE Trans. Signal Process.*, vol. 43, no. 8, pp. 1923–1935, Aug. 1995.

[6] K. T. Wong and M. D. Zoltowski, "Uni-vector-sensor ESPRIT for multi-source azimuth, elevation, and polarization estimation," *IEEE Trans. Antennas Propag.*, vol. 45, no. 10, pp. 1467–1474, Oct. 1997.

[7] K.-C. Ho, K.-C. Tan, and B. T. G. Tan, "Efficient method for estimating directions-of-arrival of partially polarized signals with electromagnetic vector sensors," *IEEE Trans. Signal Process.*, vol. 45, no. 10, pp. 2485–2498, Oct. 1997.

[8] Q. Cheng and Y. Hua, "Comment on "direction and polarization estimation using arrays with small loops and short dipoles"," *IEEE Trans. Antennas Propag.*, vol. 46, no. 3, p. 461, Mar. 1998.

[9] P.-H. Chua, C.-M. S. See, and A. Nehorai, "Vector-sensor array processing for estimating angles and times of arrival of multipath communication signals," in *Proc. IEEE Int. Conf. Acoust., Speech Signal Process.*, 1998, vol. 6, pp. 3325–3328.

[10] K.-C. Ho, K.-C. Tan, and A. Nehorai, "Estimating directions of arrival of completely and incompletely polarized signals with electromagnetic vector sensors," *IEEE Trans. Signal Process.*, vol. 47, no. 10, pp. 2845–2852, Oct. 1999.

[11] A. Nehorai and P. Tichavský, "Cross-product algorithms for source tracking using an EM vector sensor," *IEEE Trans. Signal Process.*, vol. 47, no. 10, pp. 2863–2867, Oct. 1999.

[12] K. T. Wong and M. D. Zoltowski, "Closed-form direction-finding with arbitrarily spaced electromagnetic vector-sensors at unknown locations," *IEEE Trans. Antennas Propag.*, vol. 48, no. 5, pp. 671–681, May 2000.

[13] M. D. Zoltowski and K. T. Wong, "ESPRIT-based 2D direction finding with a sparse array of electromagnetic vector-sensors," *IEEE Trans. Signal Process.*, vol. 48, no. 8, pp. 2195–2204, Aug. 2000.

[14] M. D. Zoltowski and K. T. Wong, "Closed-form eigenstructure-based direction finding using arbitrary but identical subarrays on a sparse uniform rectangular array grid," *IEEE Trans. Signal Process.*, vol. 48, no. 8, pp. 2205–2210, Aug. 2000.

[15] K. T. Wong and M. D. Zoltowski, "Self-initiating MUSIC direction finding and polarization estimation in spatio-polarizational beamspace," *IEEE Trans. Antennas Propag.*, vol. 48, no. 8, pp. 1235–1245, Aug. 2000.

[16] K. T. Wong, "Geolocation/beamforming for multiple wideband-FFH with unknown hop-sequences," *IEEE Trans. Aerosp. Electron. Syst.*, vol. 37, no. 1, pp. 65–76, Jan. 2001.
[17] K. T. Wong, "Direction finding/polarization estimation—Dipole and/or loop triad(s)," *IEEE Trans. Aerosp. Electron. Syst.*, vol. 37, no. 2, pp. 679–684, Apr. 2001.
[18] H. L. Van Trees, *Detection, Estimation, and Modulation Theory, Part IV: Optimum Array Processing*. New York: Wiley, 2002.
[19] C. C. Ko, J. Zhang, and A. Nehorai, "Separation and tracking of multiple broadband sources with one electromagnetic vector sensor," *IEEE Trans. Aerosp. Electron. Syst.*, vol. 38, no. 3, pp. 1109–1116, Jul. 2002.
[20] C.-M. S. See and A. Nehorai, "Source localization with distributed electromagnetic component sensor array processing," in *Proc. Int. Symp. Signal Process. Its Appl.*, 2003, vol. 1, pp. 177–180.
[21] X. You-Gen and L. Zhi-Wen, "Simultaneous estimation of 2-D DOA and polarization of multiple coherent sources using an electromagnetic vector sensor array," *J. China Inst. Commun.*, vol. 25, no. 5, pp. 28–38, May 2004.
[22] N. Le Bihan and J. Mars, "Singular value decomposition of quaternion matrices: A new tool for vector-sensor signal processing," *Signal Process.*, pp. 1177–1199, Jul. 2004.
[23] D. Rahamim, J. Tabrikian, and R. Shavit, "Source localization using vector sensor array in a multipath environment," *IEEE Trans. Signal Process.*, vol. 52, no. 11, pp. 3096–3103, Apr. 2006.
[24] K. T. Wong, L. Li, and M. D. Zoltowski, "Root-MUSIC-based direction-finding & polarization-estimation using diversely-polarized possibly-collocated antennas," *IEEE Antennas Wireless Propag. Lett.*, vol. 3, no. 8, pp. 129–132, 2004.
[25] Y. G. Xu and Z. W. Liu, "Regularized ESPRIT-based direction finding and polarization estimation with one electromagnetic vector sensor," in *Proc. Int. Conf. Signal Process.*, 2004, pp. 399–402.
[26] L. Wang, G. Liao, and H. Wang, "A new method for estimation of gain and phase uncertainty of an electromagnetic vector sensor," in *Proc. IEEE Int. Symp. Microw., Antennas, Propag. EMC Technol. Wireless Commun.*, 2005, pp. 712–715.
[27] X. You-Gen, L. Zhi-Wen, and Y. Guang-Xiang, "Uni-vector-sensor SOS/HOS-CSS for wide-band non-Gaussian source direction finding," in *Proc. IEEE Int. Symp. Microw., Antennas, Propag. EMC Technol. for Wireless Commun.*, 2005, pp. 855–858.
[28] S. Miron, N. Le Bihan, and J. I. Mars, "Quaternion-MUSIC for vector-sensor array processing," *IEEE Trans. Signal Process.*, vol. 54, no. 4, pp. 1218–1229, Apr. 2006.
[29] F. Ji and S. Kwong, "Frequency and 2D angle estimation based on a sparse uniform array of electromagnetic vector sensors," *EURASIP J. Appl. Signal Process.*, vol. 2006, no. 13, 2006.
[30] Y. Xu and Z. Liu, "On single-vector-sensor direction finding for linearly polarized sources having non-circular constellations," in *Proc. Int. Conf. Signal Process.*, 2006.
[31] L. Zhou and W. Li, "Partial discharge sources detection and location with an electromagnetic vector sensor," in *Proc. IEEE Conf. Indust. Electron. Appl.*, 2006.
[32] Q. Zhang, L. Wang, Y. Wang, and J.-C. Huang, "Cyclostationarity-based DOA and polarization estimation for multipath signals with a uniform linear array of electromagnetic vector sensors," in *Proc. Int. Conf. Machine Learn. Cybern.*, 2006, pp. 2047–2052.
[33] X. Gong, Y. Xu, and Z. Liu, "On the equivalence of tensor-MUSIC and matrix-MUSIC," in *Proc. Int. Symp. Antennas, Propag. EM Theory*, 2006, pp. 26–29.
[34] M. Hurtado and A. Nehorai, "Performance analysis of passive low-grazing-angle source localization in maritime environments using vector sensors," *IEEE Trans. Aerosp. Electron. Syst.*, vol. 43, no. 2, pp. 780–789, Apr. 2007.
[35] Y. Xu and Z. Liu, "Polarimetric angular smoothing algorithm for an electromagnetic vector-sensor array," *IET Radar, Sonar Navig.*, vol. 1, no. 3, pp. 230–240, Jun. 2007.
[36] N. Le Bihan, S. Miron, and J. Mars, "MUSIC algorithm for vector-sensors array using biquaternions," *IEEE Trans. Signal Process.*, vol. 55, no. 9, pp. 4523–4533, Sep. 2007.
[37] H. Kwak, E. Yang, and J. Chun, "Vector sensor arrays in DOA estimation for the low angle tracking," in *Proc. Int. Waveform Diversity Design Conf.*, 2007, pp. 183–187.
[38] L. Lo Monte, B. Elnour, D. Erricolo, and A. Nehorai, "Design and realization of a distributed vector sensor for polarization diversity applications," in *Proc. Int. Waveform Diversity Design Conf.*, 2007, pp. 358–361.
[39] L. Lo Monte, B. Elnour, and D. Erricolo, "Distributed 6D vector antennas design for direction of arrival application," in *Proc. IEEE Int. Conf. Electromagn. Adv. Appl.*, 2007, pp. 431–434.
[40] S. Hongyan, H. Hong, and S. Yaowu, "Novel solution of direction finding and polarization estimation of multipath cyclostationary signals," in *Proc. Int. Conf. Innovative Comput., Inf. Contr.*, 2007, p. 564.
[41] X. Gong, Z. Liu, and Y. Xu, "Quad-quaternion MUSIC for DOA estimation using electromagnetic vector sensors," *EURASIP J. Adv. Signal Process.*, vol. 2008, pp. 1–14, 2008.
[42] X. Shi and Y. Wang, "Parameter estimation of distributed sources with electromagnetic vector sensors," in *Proc. Int. Conf. Signal Process.*, 2008, pp. 203–206.
[43] Z. Xin, S. Yaowu, and Y. Wenhong, "2-D DOA and polarization estimation of LFM signals with one electromagnetic vector sensor," in *Proc. Int. Conf. Signal Process.*, 2008, pp. 386–389.
[44] Z. Xin, S. Yaowu, G. Hongzhi, and L. Jun, "Parameter estimation of wideband cyclostationary sources based on uni-vector-sensor," in *Chinese Control Conf.*, 2008, pp. 298–302.
[45] F. Ji, C. C. Fung, S. Kwong, and C.-W. Kok, "Joint frequency and 2-D angle estimation based on vector sensor array with sub-Nyquist temporal sampling," in *Proc. Eur. Signal Process. Conf.*, 2008.
[46] C.-Y. Chiu, J.-B. Yan, R. D. Murch, J. X. Yun, and R. G. Vaughan, "Design and implementation of a compact 6-port antenna," *IEEE Antennas Wireless Propag. Lett.*, vol. 8, pp. 767–770, 2009.
[47] X. Gong, Z. Liu, Y. Xu, and M. I. Ahmad, "Direction-of-arrival estimation via twofold mode-projection," *Signal Process.*, vol. 89, pp. 831–842, Dec. 2009.

Kainam Thomas Wong (S'85–M'86–SM'01) received the B.S.E. degree in chemical engineering from the University of California, Los Angeles, in 1985, the B.S.E.E. degree from the University of Colorado, Boulder, in 1987, the M.S.E.E. degree from Michigan State University, East Lansing, in 1990, and the Ph.D. degree in electrical engineering from Purdue University, West Lafayette, IN, in 1996.

He was a manufacturing engineer at the General Motors Technical Center, Warren, MI, from 1990 to 1991, and a Senior Professional Staff Member with the Johns Hopkins University Applied Physics Laboratory, Laurel, MD, from 1996 to 1998. Between 1998 and 2006, he had been a faculty member at Nanyang Technological University (Singapore), the Chinese University of Hong Kong, and the University of Waterloo (Canada). He was conferred the *Premier's Research Excellence Award* by the Canadian province of Ontario in 2003. Since 2006, he has been with the Hong Kong Polytechnic University as an Associate Professor. His research interest includes sensor-array signal processing and signal processing for communications.

Dr. Wong has/had been an Associate Editor for *Circuits, Systems, and Signal Processing*, the IEEE SIGNAL PROCESSING LETTERS, the IEEE TRANSACTIONS ON SIGNAL PROCESSING, and the IEEE TRANSACTIONS ON VEHICULAR TECHNOLOGY.

Xin Yuan (S'09) received the B.Eng. degree in electronic information engineering in 2007 and the M.Eng. degree in information and communication engineering in 2009, both from Xidian University, Xi'an, Shaanxi, China.

He is currently working toward the Ph.D. degree at the Hong Kong Polytechnic University. His research interest lies in space-time signal processing.